Vortex Tubes in Turbulence Velocity Fields at High Reynolds Numbers

Hideaki Mouri * and Akihiro Hori **

Meteorological Research Institute, Nagamine, Tsukuba 305-0052, Japan

Abstract

The elementary structures of turbulence, i.e., vortex tubes, are studied using velocity data obtained in laboratory experiments for boundary layers and duct flows at microscale Reynolds numbers $Re_\lambda = 332$–1934. While past experimental studies focused on intense vortex tubes, the present study focuses on all vortex tubes with various intensities. We obtain the mean velocity profile. The radius scales with the Kolmogorov length. The circulation velocity scales with the Kolmogorov velocity, in contrast to the case of intense vortex tubes alone where the circulation velocity scales with the rms velocity fluctuation. Since these scaling laws are independent of the configuration for turbulence production, they appear to be universal at high Reynolds numbers.

1 Introduction

Turbulence contains vortex tubes as the elementary structures (Frisch, 1995; Sreenivasan and Antonia, 1997; Makihara *et al.*, 2002). Regions of significant vorticity tend to be organized into tubes. They occupy a small fraction of the volume and are embedded in the background fluctuation. Their existence was established at microscale Reynolds numbers $Re_\lambda \lesssim 2000$, by seeding a turbulent liquid with gas bubbles and thereby visualizing regions of low pressure that are associated with vorticity (Douady *et al.*, 1991; La Porta *et al.*, 2000).

At low Reynolds numbers, $Re_\lambda \lesssim 200$, direct numerical simulations derived basic parameters of vortex tubes. The radii are of the order of the Kolmogorov length η. The total lengths are of the order of the correlation length L. The

* Corresponding author. *E-mail address:* hmouri@mri-jma.go.jp

**Affiliated with Meteorological and Environmental Sensing Technology, Inc., Nanpeidai, Ami 300-0312, Japan

circulation velocities are of the order of the Kolmogorov velocity u_K or the rms velocity fluctuation $\langle u^2 \rangle^{1/2}$. Here $\langle \cdot \rangle$ denotes an average. The lifetimes are of the order of the turnover time for energy-containing eddies $L/\langle u^2 \rangle^{1/2}$ (Vincent and Meneguzzi, 1991, 1994; Jiménez *et al.*, 1993; Jiménez and Wray, 1998; Makihara *et al.*, 2002; Tanahashi *et al.*, 2004).

However, for most of the tube parameters, universality has not been established because the behavior has not been known at high Reynolds numbers. At $Re_\lambda \gtrsim 200$, a direct numerical simulation is not easy for now. The bubble visualization does not have a high enough spatial resolution (La Porta *et al.*, 2000), except for the study of the tube length and lifetime.

The more promising approach is velocimetry in laboratory experiments. A probe suspended in the flow is used to obtain a one-dimensional cut of the velocity field. The small-scale velocity variation is enhanced at the positions of vortex tubes. [1] In particular, the velocity component v that is perpendicular to the one-dimensional cut is suited to detecting circulation flows associated with vortex tubes (Mouri *et al.*, 1999).

Based on this approach, there were already several studies (Belin *et al.*, 1996; Noullez *et al.*, 1997; Camussi and Guj, 1999). Recently, using boundary layers at $Re_\lambda = 332$–1304 and duct flows at $Re_\lambda = 719$–1934, we studied the mean radius R_0 and circulation velocity V_0 of vortex tubes and obtained the scalings $R_0 \propto \eta$ and $V_0 \propto \langle v^2 \rangle^{1/2}$ (Mouri *et al.*, 2007). However, this and other past studies focused on intense vortex tubes that are easily captured by imposing a threshold on the velocity variation. For all vortex tubes with various intensities, the tube parameters have not been known. Now we try to study vortex tubes as a whole.

2 Experimental Data

The present study is based on data of our past experiments described in Mouri *et al.* (2007). Since wide ranges of the Reynolds number Re_λ were obtained in two configurations for turbulence production, i.e., boundary layer and duct flow, we are able to study dependence of tube parameters on the Reynolds number and on the large-scale flow. Since the data were long, (1–4) $\times 10^8$ points, their statistics are expected to be significant. Table 1 lists turbulence parameters that are to be used here.

[1] Other vortical structures, i.e., vortex sheets, are not important at least statistically. This is already known for the case of intense velocity variation (Noullez *et al.*, 1997; Mouri *et al.*, 2007) and is to be demonstrated here for the case of velocity variation with arbitrary intensity (§4).

Table 1
Turbulence parameters in boundary layers (B1–B6) and duct flows (D1–D5): sampling interval δx_s, Kolmogorov length $\eta = (\nu^3/\langle\varepsilon\rangle)^{1/4}$ where ν is the kinematic viscosity and $\langle\varepsilon\rangle = 15\nu\langle(\partial_x v)^2\rangle/2$ is the mean energy dissipation rate, Taylor microscale $\lambda = [2\langle v^2\rangle/\langle(\partial_x v)^2\rangle]^{1/2}$, Kolmogorov velocity $u_K = (\nu\langle\varepsilon\rangle)^{1/4}$, rms velocity fluctuations $\langle u^2\rangle^{1/2}$ and $\langle v^2\rangle^{1/2}$, and microscale Reynolds number $Re_\lambda = \lambda\langle v^2\rangle^{1/2}/\nu$. The parameter values are from Mouri *et al.* (2007).

Data	δx_s [cm]	η [cm]	λ [cm]	u_K [m/s]	$\langle u^2\rangle^{1/2}$ [m/s]	$\langle v^2\rangle^{1/2}$ [m/s]	Re_λ
B1	0.0378	0.0539	1.93	0.0262	0.283	0.242	332
B2	0.0312	0.0335	1.46	0.0423	0.582	0.475	488
B3	0.0265	0.0198	1.04	0.0716	1.18	0.973	716
B4	0.0230	0.0152	0.919	0.0934	1.80	1.46	945
B5	0.0180	0.0120	0.776	0.118	2.46	1.98	1080
B6	0.0184	0.0104	0.742	0.137	3.14	2.51	1304
D1	0.0355	0.0288	1.52	0.0489	0.694	0.666	719
D2	0.0255	0.0177	1.15	0.0798	1.38	1.34	1098
D3	0.0217	0.0133	0.986	0.107	2.11	2.04	1416
D4	0.0216	0.0111	0.895	0.128	2.84	2.69	1693
D5	0.0212	0.00955	0.826	0.149	3.46	3.32	1934

The experiments were done in a wind tunnel of the Meteorological Research Institute. We use coordinates x, y, and z in the streamwise, spanwise, and floor-normal directions. The origin $x = y = z = 0$ m is on the tunnel floor at the entrance to the test section. Its size was $\delta x = 18$ m, $\delta y = 3$ m, and $\delta z = 2$ m. We simultaneously measured the velocity fluctuations u and v in the streamwise and spanwise directions, by using a hot-wire anemometer with a crossed-wire probe. The wires were 5 μm in diameter, 1.25 mm in sensing length, 1.4 mm in separation, and oriented at $\pm 45°$ to the streamwise direction. Taylor's frozen-flow hypothesis was used to convert temporal variations into spatial variations. The sampling interval δx_s was set to be as small as possible, on the condition that high-wave-number noise was not significant in the power spectrum.

2.1 Boundary Layers (Data B1–B6)

Over the entire floor of the tunnel test section, we placed blocks as roughness elements. Their size was $\delta x = 0.06$ m, $\delta y = 0.21$ m, and $\delta z = 0.11$ m. Their

spacing was $\delta x = \delta y = 0.5$ m. The measurement position was at $x = 12.5$ m, where the boundary layer had been well developed, and $z = 0.25$–0.35 m in the log-law sublayer.[2] We obtained the data B1–B6 at $Re_\lambda = 332$–1304 by changing the incoming-flow velocity from 2 to 20 m s^{-1}.

2.2 Duct Flows (Data D1–D5)

At $x = -2$ m, we placed a rectangular duct with width $\delta y = 1.3$ m and $\delta z = 1.4$ m. The duct center was on the tunnel axis. The measurement position was at $x = 15.5$ m and $z = 0.6$ m, where the flow had become turbulent. We obtained the data D1–D5 at $Re_\lambda = 719$–1934 by changing the duct-exit flow velocity from 11 to 55 m s^{-1}.

3 Model for Vortex Tubes

Using the Burgers vortex, an idealized model for vortex tubes, we discuss what information is available from a one-dimensional cut of the velocity field (for a similar discussion based on a direct numerical simulation, see Mouri *et al.* (1999)). The Burgers vortex is an axisymmetric steady circulation in a strain field. In cylindrical coordinates, the circulation u_Θ and strain field (u_R, u_Z) are

$$u_\Theta \propto \frac{\nu}{a_0 R}\left[1 - \exp\left(-\frac{a_0 R^2}{4\nu}\right)\right] \quad \text{and} \quad (u_R, u_Z) = \left(-\frac{a_0 R}{2}, a_0 Z\right). \qquad (1)$$

Here ν is the kinematic viscosity and a_0 (> 0) is a constant. The circulation is maximal at $R = R_0 = 2.24(\nu/a_0)^{1/2}$. Thus, R_0 is regarded as the tube radius. We do not use other models for vortex tubes, e.g., spirals of Lundgren (1982), because detailed information about individual vortex tubes is anyway not available from one-dimensional velocity data.

Suppose that velocity data are obtained on a one-dimensional cut of a flow field that consists of vortex tubes and the background random fluctuation, as illustrated in Fig. 1a. The one-dimensional cut is along the x axis, the tube

[2] The measurement position might appear to have been too close to the floor of the tunnel, but this is not serious at all. First, this is not in contradiction to our purpose, which is to find features of vortex tubes that are independent of the large-scale flow. Second, not invalid is the basic assumption of our study that the spatial distribution of vortex tubes was similar among experiments (§3). Since the measured ratio $\langle u^2\rangle/\langle v^2\rangle$ is not far from unity (Table 1), the tube distribution at the measurement position should have been almost isotropic in all the experiments.

position is (x_0, y_0), and the tube inclination is (θ_0, φ_0). The circulation flows u_Θ of the vortex tubes induce small-scale variations in the v signal.

If we consider intense velocity variations above a high threshold (Mouri *et al.*, 2007), their scale and amplitude correspond to the radius and circulation velocity of intense vortex tubes with $|y_0| \lesssim R_0$ and $\theta_0 \simeq 0$. To demonstrate this, mean profiles along the cut x are obtained for the circulation flows u_Θ of the Burgers vortices with random positions (x_0, y_0) and inclinations (θ_0, φ_0). Their radii R_0 and maximum circulation velocities $V_0 = u_\Theta(R_0)$ are set to be the same. We consider the Burgers vortices with $|\partial_x v|$ at $x = 0$ being above a threshold, $|\partial_x v|/3$ for $x_0 = y_0 = \theta_0 = 0$ at $x = 0$. When $\partial_x v$ is negative, the sign of the v signal is inverted before the averaging. The result is shown in Fig. 1b. Around the peaks, the mean v profile is similar to that of the Burgers vortex for $x_0 = y_0 = \theta_0 = 0$ (dotted line).

If we consider all velocity variations that are more significant than the background fluctuation, which roughly correspond to velocity variations above a low threshold, vortex tubes with $|y_0| \gg R_0$ or $\theta_0 \gg 0$ significantly contribute to the mean v profile. Its scale is large while its amplitude is small as compared with the mean radius and circulation velocity of all vortex tubes. Nevertheless, the scale and amplitude of the mean v profile are proportional to the mean radius and circulation velocity of all vortex tubes, among flow fields where the distribution of vortex tubes is similar. This is likely in our experiments. Since the measured ratio $\langle u^2 \rangle / \langle v^2 \rangle$ is not far from unity (Table 1), the tube

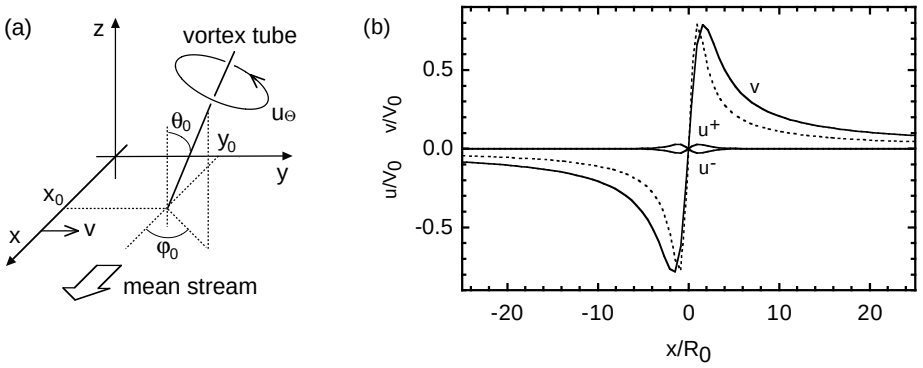

Fig. 1. (a) Sketch of a vortex tube penetrating the (x, y) plane at a point (x_0, y_0). The inclination is (θ_0, φ_0). The circulation velocity is u_Θ. We consider the spanwise velocity v along the x axis in the mean stream direction. (b) Mean profiles for the Burgers vortices with random positions and inclinations. The streamwise velocity u is separately shown for $\partial_x u > 0$ (u^+) and $\partial_x u \leq 0$ (u^-) at $x = 0$. The position and velocities are normalized by the radius R_0 and maximum circulation velocity V_0 of the Burgers vortices. The dotted line is the v profile of the Burgers vortex for $x_0 = y_0 = \theta_0 = 0$, the peak value of which is scaled to that of the mean v profile.

inclination (θ_0, φ_0) should have been random in all the experiments. Then, we are able to study dependence of those tube parameters on the Reynolds number Re_λ and on the configuration for turbulence production.

4 Mean Velocity Profile

The spanwise-velocity increment $v(x+\delta x_0/2)-v(x-\delta x_0/2)$ over a small scale δx_0 varies at the position $x = x_0$ of a vortex tube, regardless of its intensity. We try to use all of such variations and study vortex tubes as a whole. The increment is smoothed with the Gaussian window function $\exp(-x^2/2\delta x_0^2)$. We determine the tube positions x_0 as local maxima and minima of the smoothed increment and then analyze the unsmoothed velocity data. The smoothing is to make sure that each of the local maxima and minima corresponds to each vortex tube. Also, the smoothing reduces the background fluctuation. We set δx_0 to be a multiple of the sampling interval δx_s that is close to the mean radius 6η estimated for intense vortex tubes in Mouri *et al.* (2007). This estimate is consistent with those in Jiménez *et al.* (1993), Belin *et al.* (1996), Jiménez and Wray (1998), and Tanahashi *et al.* (2004), if we consider

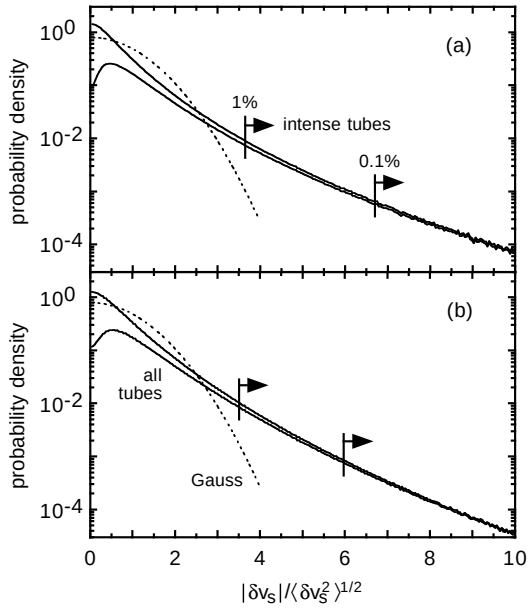

Fig. 2. Probability density of $|\delta v_s| = |v(x + \delta x_s) - v(x)|$. (a) $Re_\lambda = 719$ (D1). (b) $Re_\lambda = 1934$ (D5). We normalize $|\delta v_s|$ by $\langle \delta v_s^2 \rangle^{1/2} = \langle [v(x + \delta x_s) - v(x)]^2 \rangle^{1/2}$. The dotted line denotes the Gaussian distribution. The arrows indicate the ranges for intense vortex tubes studied by Mouri *et al.* (2007), which share 0.1 and 1% of the total. We also show the probability density for all vortex tubes.

the difference in the definition of tube radius.

Fig. 2 compares the probability density of the absolute velocity increment $|v(x+\delta x_s)-v(x)|$ over the sampling interval δx_s for the entire data with that for the subdata from $x = x_0-\delta x_0$ to $x_0+\delta x_0-\delta x_s$ around all tube positions x_0. The latter distribution accounts for the tail of the former distribution where vortex tubes should be dominant (Mouri *et al.*, 2007), and does not account for the center of the former distribution where the background fluctuation should be dominant. It is thereby expected that we have surely captured vortex tubes.

Fig. 3 shows the mean velocity profiles obtained by averaging signals centered at individual tube positions x_0. The v profile is similar to that in Fig. 1b. Hence, the contribution from vortex tubes is surely dominant. The contribution from vortex sheets is not dominant. If it were dominant, the v profile in Fig. 3 should exhibit some kind of step (Noullez *et al.*, 1997; Mouri *et al.*, 2007). Exceptionally, to the extended tails of the v profile, the contribution from vortex sheets might be dominant.

By fitting the v profile in Fig. 3 around its peaks by the v profile of the Burgers vortex for $x_0 = y_0 = \theta_0 = 0$ (dotted line), we estimate the radius R_0

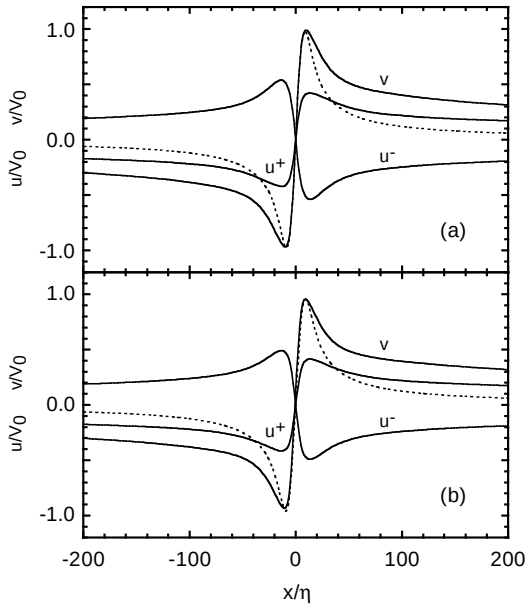

Fig. 3. Mean profiles of all vortex tubes in the streamwise (u) and spanwise (v) velocities. (a) $Re_\lambda = 719$ (D1). (b) $Re_\lambda = 1098$ (D2). The u profile is separately shown for $\partial_x u > 0$ (u^+) and $\partial_x u \le 0$ (u^-) at $x = 0$. The dotted line is the v profile fitted by the Burgers vortex for $x_0 = y_0 = \theta_0 = 0$. Its V_0 value is used to normalize the velocities. The position x is normalized by the Kolmogorov length η. For the corresponding figure for intense vortex tubes alone, see Fig. 4 of Mouri *et al.* (2007).

Table 2
Parameters of vortex tubes in boundary layers (B1–B6) and duct flows (D1–D5): identification scale δx_0, radius R_0, maximum circulation velocity V_0, and Reynolds number $Re_0 = R_0 V_0/\nu$. For parameters of intense vortex tubes alone, see Table 2 of Mouri *et al.* (2007).

Data	$\delta x_0/\eta$	R_0/η	V_0/u_K	$V_0/\langle v^2\rangle^{1/2}$	Re_0	$Re_0/Re_\lambda^{1/2}$
B1	6.30	8.45	2.43	0.263	20.5	1.13
B2	5.59	8.47	2.39	0.213	20.2	0.914
B3	5.36	8.59	2.47	0.182	21.2	0.792
B4	6.06	9.21	2.73	0.175	25.1	0.817
B5	6.00	8.93	2.83	0.169	25.3	0.770
B6	5.30	8.28	2.88	0.157	23.8	0.659
D1	6.16	8.56	2.43	0.179	20.8	0.776
D2	5.76	8.91	2.56	0.152	22.8	0.688
D3	6.52	9.12	2.79	0.146	25.4	0.675
D4	5.84	8.72	2.91	0.138	25.4	0.617
D5	6.66	8.81	3.18	0.143	28.0	0.637

and maximum circulation velocity V_0. The measured velocity is considered to have been smoothed over the probe size in the streamwise direction, 1 mm. Table 2 lists the R_0 and V_0 values. While the R_0 value is greater than the true mean radius, the V_0 value is less than the true mean circulation velocity, because of the contribution from vortex tubes with $|y_0| \gg R_0$ or $\theta_0 \gg 0$. The R_0 and V_0 values are still proportional to the true mean values (§3).

The u profile in Fig. 3 is separated for $\partial_x u > 0$ (u^+) and $\partial_x u \leq 0$ (u^-) at $x = 0$.[3] These $u^\pm$ profiles have larger amplitudes than the $u^\pm$ profiles in Fig. 1b. This is a signature of vortex tubes with $|y_0| \gg R_0$ or $\theta_0 \gg 0$, especially of tubes passing the probe with some incidence angles relative to

[3] We have decomposed the $u^\pm$ profiles into symmetric and antisymmetric components and show only the antisymmetric components (Mouri *et al.*, 2007). This is because, although the $u^\pm$ profiles for vortex tubes should be antisymmetric, a symmetric positive excursion is induced by the contamination with the w velocity that is perpendicular to the u and v velocities (Sassa and Makita, 2005). The two wires of the hot-wire anemometer individually respond to all the u, v, and w velocities. Since the measured u velocity corresponds to the sum of the responses of the two wires, it is contaminated with the w velocity. Since the measured v velocity corresponds to the difference of the responses, it is free from the w velocity.

the mean flow direction, $\tan^{-1}[v/(U+u)]$ (Belin *et al.*, 1996). The radial inflow u_R of the strain field is not discernible, except that the u^- profile has a larger amplitude than the u^+ profile. Unlike the Burgers vortex, a real vortex tube is not always oriented to the stretching direction (Vincent and Meneguzzi, 1991, 1994; Jiménez *et al.*, 1993; Jiménez and Wray, 1998; Tanahashi *et al.*, 2004).

5 Scaling Laws of Tube Parameters

The dependence of tube parameters on the microscale Reynolds number Re_λ and on the configuration for turbulence production, i.e., boundary layer or duct flow, is studied in Fig. 4. Each quantity was normalized by its value in the duct flow at $Re_\lambda = 1934$ (D5). That is, we avoid the prefactors that are not equal to the true values (§4). We instead focus on scaling laws.

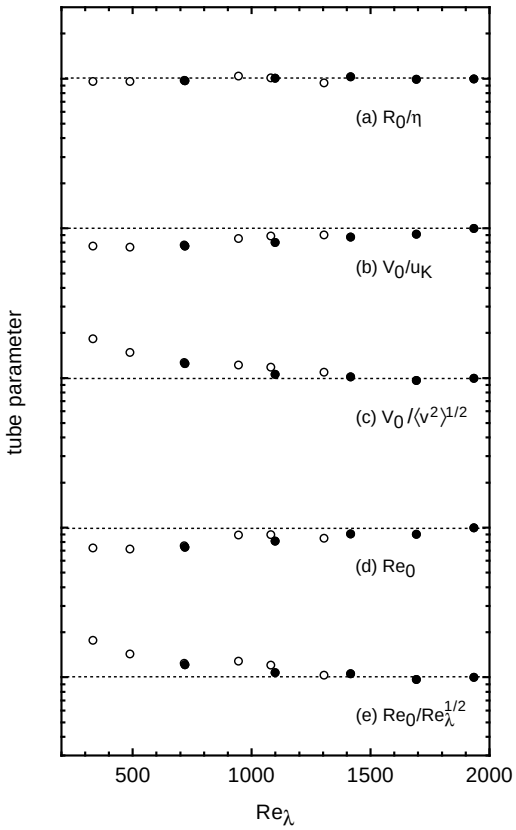

Fig. 4. Dependence of parameters of all vortex tubes on Re_λ. (a) R_0/η. (b) V_0/u_K. (c) $V_0/\langle v^2\rangle^{1/2}$. (d) Re_0. (e) $Re_0/Re_\lambda^{1/2}$. The open circles denote the boundary layers (B1–B6). The filled circles denote the duct flows (D1–D5). Each quantity is normalized by its value in the duct flow at $Re_\lambda = 1934$ (D5). For the corresponding figure for intense vortex tubes alone, see Fig. 7 of Mouri *et al.* (2007).

The radius R_0 scales with the Kolmogorov length η as $R_0 \propto \eta$ (Fig. 4a). This is partly because vortex tubes were identified on a scale $\delta x_0 \simeq 6\eta$ (§4), but the scatter of R_0/η is less than the scatter of $\delta x_0/\eta$ as in Table 2.

The maximum circulation velocity V_0 scales with the Kolmogorov velocity u_K as $V_0 \propto u_K$ (Fig. 4b) rather than with the rms velocity fluctuation $\langle v^2 \rangle^{1/2}$ as $V_0 \propto \langle v^2 \rangle^{1/2}$ (Fig. 4c), if we consider the entire Re_λ range. This result is reasonable because u_K is a characteristic of small-scale motions. At $Re_\lambda \gtrsim 1000$, the scaling $V_0 \propto \langle v^2 \rangle^{1/2}$ is also significant. Since $V_0 \propto \langle v^2 \rangle^{1/2}$ is observed for intense vortex tubes (§6), $V_0 \propto \langle v^2 \rangle^{1/2}$ is also observed for all vortex tubes if the mean v profile is biased toward intense vortex tubes. This is more likely at higher Re_λ because $Re_\lambda \propto \langle v^2 \rangle / u_K^2$. However, since intense vortex tubes are rare (§6), $V_0 \propto \langle v^2 \rangle^{1/2}$ does not represent vortex tubes as a whole. We do not consider the scaling $V_0 \propto \langle v^2 \rangle^{1/2}$.

Direct numerical simulations of homogeneous isotropic turbulence and turbulent channel flows at $Re_\lambda \lesssim 200$ derived the scalings $R_0 \propto \eta$ and $V_0 \propto u_K$ for all vortex tubes (Makihara *et al.*, 2002; Tanahashi *et al.*, 2004). We have found that, regardless of the configuration for turbulence production, those scalings extend at least up to $Re_\lambda \simeq 2000$.

The scalings of the radius R_0 and circulation velocity V_0 lead to a scaling of the Reynolds number $Re_0 = R_0 V_0/\nu$ that characterizes stability of vortex tubes (Jiménez *et al.*, 1993; Jiménez and Wray, 1998):

$$Re_0 = \text{constant} \quad \text{if } R_0 \propto \eta \text{ and } V_0 \propto u_K, \tag{2a}$$

$$Re_0 \propto Re_\lambda^{1/2} \quad \text{if } R_0 \propto \eta \text{ and } V_0 \propto \langle v^2 \rangle^{1/2} \tag{2b}$$

If we consider the entire Re_λ range, our result favors the former scaling (Fig. 4d) rather than the latter (Fig. 4e). This is in accordance with the observed scalings of R_0 and V_0 (Figs. 4a and 4b). The constancy of Re_0 implies that vortex tubes as a whole are stable against an increase of the Reynolds number Re_λ. At $Re_\lambda \gtrsim 1000$, the scaling $Re_0 \propto Re_\lambda^{1/2}$ is also significant. This scaling is not important to us because it is related with $V_0 \propto \langle v^2 \rangle^{1/2}$ discussed before (Fig. 4c).

6 Comparison with Intense Vortex Tubes

The present result for all vortex tubes with various intensities is compared with a past result for intense vortex tubes alone. We use the result of Mouri *et al.* (2007), which was based on the same experimental data. For a similar experimental result for intense vortex tubes, see Belin *et al.* (1996).

To identify intense vortex tubes, Mouri *et al.* (2007) imposed a threshold on the absolute velocity increment $|v(x+\delta x_s)-v(x)|$. The threshold was such that 0.1% or 1% of the increments were used for the identification. These increments are included in the increments used for all vortex tubes as shown in Fig. 2. Thus, intense vortex tubes studied by Mouri *et al.* (2007) are included in all vortex tubes studied here.

Mouri *et al.* (2007) estimated the radius R_0 and maximum circulation velocity V_0 from mean velocity profiles. They were obtained by averaging signals centered at individual positions where $|v(x+\delta x_s)-v(x)|$ was above the threshold. Since the mean velocity profiles were dominated by vortex tubes with $|y_0| \lesssim R_0$ and $\theta_0 \simeq 0$, the R_0 and V_0 values are close to the true mean radius and true mean circulation velocity (§3). The dependence of R_0 and V_0 on the threshold was discussed in Mouri *et al.* (2007).

The radius for intense vortex tubes, $R_0/\eta \simeq 5$–7 (Mouri *et al.*, 2007), is less than that for all vortex tubes, $R_0/\eta \simeq 8$–9 (Table 2). While the former is close to the true mean radius, the latter is greater than the true mean radius (§4). The true mean radius appears not to be significantly different between intense and all vortex tubes. Both of them obey the scaling $R_0 \propto \eta$. The circulation flows of vortex tubes are always of smallest scales of turbulence.

The circulation velocity for intense vortex tubes, $V_0/\langle v^2\rangle^{1/2} \simeq 0.4$–$0.8$ (Mouri *et al.*, 2007), is greater than that for all vortex tubes, $V_0/\langle v^2\rangle^{1/2} \simeq 0.1$–$0.3$ (Table 2). This is mainly due to the difference in the true mean circulation velocity. In addition, the V_0 value for all vortex tubes is less than the true mean circulation velocity (§4). While all vortex tubes obey the scaling $V_0 \propto u_K$, intense vortex tubes obey the scaling $V_0 \propto \langle v^2\rangle^{1/2}$ in the same Re_λ range.

The Reynolds number for intense vortex tubes scales as $Re_0 \propto Re_\lambda^{1/2}$, which is explained through equation (2b) by the scalings $R_0 \propto \eta$ and $V_0 \propto \langle v^2\rangle^{1/2}$. With an increase of Re_λ, intense vortex tubes progressively have higher Re_0 and are more unstable. The situation is different in the case of all vortex tubes, for which Re_0 is constant.

Direct numerical simulations at $Re_\lambda \lesssim 200$ derived $R_0 \propto \eta$, $V_0 \propto \langle v^2\rangle^{1/2}$, and hence $Re_0 \propto Re_\lambda^{1/2}$ for intense vortex tubes (Jiménez *et al.*, 1993; Jiménez and Wray, 1998) while $R_0 \propto \eta$, $V_0 \propto u_K$, and hence $Re_0 =$ constant for all vortex tubes (Makihara *et al.*, 2002; Tanahashi *et al.*, 2004). This difference in the scalings of V_0 and Re_0 is the same as that obtained here up to $Re_\lambda \simeq 2000$.

The difference in the scalings of V_0 and Re_0 between intense and all vortex tubes implies that their roles are different. Since $V_0 \propto \langle v^2\rangle^{1/2}$, intense vortex tubes are responsible for small-scale intermittency. This is especially the case at high Re_λ because $Re_\lambda \propto \langle v^2\rangle/u_K^2$. In fact, at high Re_λ, small-

scale intermittency is significant. However, since $Re_0 \propto Re_\lambda^{1/2}$, intense vortex tubes have short lifetimes and thus rare at high Re_λ (Jiménez *et al.*, 1993; Jiménez and Wray, 1998; Mouri *et al.*, 2007). On the other hand, vortex tubes as a whole obey the scalings $V_0 \propto u_K$ and $Re_0 =$ constant. They are always ubiquitous and responsible for an important fraction of energy at smallest scales.

7 Conclusion

Using velocity data obtained in boundary layers at $Re_\lambda = 332$–1304 and duct flows at $Re_\lambda = 719$–1934 (Mouri *et al.*, 2007), we have studied vortex tubes, i.e., the elementary structures of turbulence. While past experimental studies focused on intense vortex tubes, the present study focuses on all vortex tubes with various intensities. We have obtained the mean velocity profile, estimated the radius R_0 and maximum circulation velocity V_0, and then obtained the scalings $R_0 \propto \eta$, $V_0 \propto u_K$, and $Re_0 = R_0 V_0/\nu =$ constant. They are in contrast to the scalings for intense vortex tubes alone, i.e., $R_0 \propto \eta$, $V_0 \propto \langle v^2 \rangle^{1/2}$, and $Re_0 \propto Re_\lambda^{1/2}$. Since those scalings for all vortex tubes are independent of the configuration for turbulence production, they appear to be universal at high Reynolds numbers Re_λ. The implication of the scalings is that vortex tubes as a whole are always ubiquitous and responsible for an important fraction of energy at smallest scales.

The present study has some ambiguities because only one-dimensional data of the velocity field are available. To proceed further, two- or three-dimensional velocity data are necessary but are not available for now. The advent of array of hot-wire probes (Sassa and Makita, 2005) or particle image velocimeter (Tanahashi *et al.*, 2002) that is applicable to vortex tubes at high Reynolds numbers is desirable. Such a technique would enlarge our knowledge of vortex tubes. For example, the study of the probability density distributions of the tube radius and maximum circulation velocity is of interest.

References

Belin, F., Maurer, J., Tabeling, P. and Willaime, H. 1996. Observation of intense filaments in fully developed turbulence. J. Phys. (Paris) II 6, 573–584.

Camussi, R. and Guj, G. 1999. Experimental analysis of intermittent coherent structures in the near field of a high Re turbulent jet flow. Phys. Fluids 11, 423–431.

Douady, S., Couder, Y. and Brachet, M.E. 1991. Direct observation of the

intermittency of intense vorticity filaments in turbulence. Phys. Rev. Lett. 67, 983–986.

Frisch, U. 1995. Turbulence, the Legacy of A.N. Kolmogorov. Cambridge Univ. Press, Cambridge.

Jiménez, J. and Wray, A.A. 1998. On the characteristics of vortex filaments in isotropic turbulence. J. Fluid Mech. 373, 255–285.

Jiménez, J., Wray, A.A., Saffman, P.G. and Rogallo, R.S. 1993. The structure of intense vorticity in isotropic turbulence. J. Fluid Mech. 255, 65–90.

La Porta, A., Voth, G.A., Moisy, F. and Bodenschatz, E. 2000. Using cavitation to measure statistics of low-pressure events in large-Reynolds-number turbulence. Phys. Fluids 12, 1485–1496.

Lundgren, T.S. 1982. Strained spiral vortex model for turbulent fine structure. Phys. Fluids 25, 2193–2203.

Makihara, T., Kida, S. and Miura, H. 2002. Automatic tracking of low-pressure vortex. J. Phys. Soc. Jpn. 71, 1622–1625.

Mouri, H., Hori, A. and Kawashima, Y. 2007. Laboratory experiments for intense vortical structures in turbulence velocity fields. Phys. Fluids 19, 055101.

Mouri, H., Takaoka, M. and Kubotani, H. 1999. Wavelet identification of vortex tubes in a turbulence velocity field. Phys. Lett. A 261, 82–88.

Noullez, A., Wallace, G., Lempert, W., Miles, R.B. and Frisch, U. 1997. Transverse velocity increments in turbulent flow using the RELIEF technique. J. Fluid Mech. 339, 287–307.

Sassa, K. and Makita, H. 2005. Reynolds number dependence of elementary vortices in turbulence. In: Rodi, W. and Mulas, M. (Ed.), Engineering Turbulence Modelling and Experiments 6. Elsevier, Oxford, pp. 431–440.

Sreenivasan, K.R. and Antonia, R.A. 1997. The phenomenology of small-scale turbulence. Annu. Rev. Fluid Mech. 29, 435–472.

Tanahashi, M., Kang, S.-J., Miyamoto, T., Shiokawa, S. and Miyauchi, T. 2004. Scaling law of fine scale eddies in turbulent channel flows up to $Re_\tau = 800$. Int. J. Heat Fluid Flow 25, 331–340.

Tanahashi, M., Ootsu, M., Fukushima, M. and Miyauchi, T. 2002. Measurement of coherent fine scale eddies in turbulent mixing layer by DPIV. In: Rodi, W. and Fueyo, N. (Ed.), Engineering Turbulence Modelling and Experiments 5. Elsevier, Oxford, pp. 525–534.

Vincent, A. and Meneguzzi, M. 1991. The spatial structure and statistical properties of homogeneous turbulence. J. Fluid Mech. 225, 1–20.

Vincent, A. and Meneguzzi, M. 1994. The dynamics of vorticity tubes in homogeneous turbulence. J. Fluid Mech. 258, 245–254.